Study of Long-Duration Flares and Associated Chromospheric and Coronal Ejections in Solar Cycles 23 and 24

A. N. Shakhovskaya[a], * and I. Yu. Grigor'eva[b], *

[a]*Crimean Astrophysical Observatory, Russian Academy of Sciences, Nauchnij, Republic of Crimea, Russia*
[b]*Central Astronomical Observatory of the Russian Academy of Sciences at Pulkovo, St. Petersburg, Russia*
*e-mail: anshakh@yandex.ru
**e-mail: irina.2014.irina@mail.ru

Abstract—A statistical study of long-duration (long-duration event, LDE) flares in the soft X-ray (SXR) range for solar cycles 23 and 24 is carried out. Graphs of the dependence of the strength of LDE flares and coronal mass ejections (CMEs) on the duration of these flares are constructed. As a result, we find that a significant proportion of LDE flares is not associated with large mass CMEs. This contradicts the hypothesis that the energy required to maintain the post-eruptive phase of LDE flares is supplied by the energy of settling matter after CME eruption. However, most flares are accompanied by mini-eruptions, which may have a significance in the energy balance of LDEs. The diagram of the strength–duration of flares shows that there is a limit of energy and maximum strength of an LDE flare in the SXR range in LDE events. Apparently, this limit differs for cycles 23 and 24. This fact may indicate that there is a limit to the maximum flare energy that can be observed in a particular solar cycle.

1. INTRODUCTION

Solar flares can be divided into two significantly different classes: compact or impulsive flares and long-duration events (LDEs). It is currently believed that the development of the MHD instability of the magnetic configuration leads to chromospheric and coronal mass ejections (CMEs). Subsequent relaxation is accompanied by the reconnection of magnetic field lines and the formation of a coronal current sheet, which leads to impulse energy release and the formation of coronal loops filled with hot plasma (Gopalswamy, 2003; Grechnev et al., 2006). The SXR radiation in impulse events lasts 10–20 min, while it decays slowly for many hours in LDEs.

In this article, a flare is defined as a significant emission increase in the SXR range and chromospheric lines. Accordingly, by flare duration, we mean the duration of SXR radiation. Recall that the term *LDE* was introduced by Antalova in the late 1980s (Antalova, 1988), when regular measurements of the solar integral flux of the SXR radiation began. It is generally recognized that this requires an additional supply of energy, in addition to the release of energy in the impulse phase. One such energy source can be the settling of matter after a CME. The relationship between chromospheric ejections and CMEs and LDE flares has been discussed (Shibasaki, 2002; Shakhovskaya and Akhtemov, 2013; Shakhovskaya

et al., 2006; Livshits et al., 2013). A slight correlation (0.45) between the CME mass and the duration of SXR flares was found (Gopalswamy, 2003; Yashiro and Gopalswamy, 2009). However, there are LDE flares even without massive CMEs, and the question of additional energy remains open.

## 2. CMEs AND ASSOCIATED LDE FLARES IN CYCLE 24

A statistical analysis of all LDE flares of solar cycle 24 from the consolidated solar activity reports of the US Space Weather Prediction Center (SWPC, ftp.swpc.noaa.gov/pub/indices/events/) was carried out. Flares with a total SXR duration of >40 min and an SXR class of M1.0 or higher accompanied by CMEs were selected. There were 72 such events from 2011 to 2017. The CME mass was taken from the SOHO LASCO CME CATALOG (cdaw.gsfc.nasa.gov/CME_list/). Publicly available data from SOHO LASCO (Brueckner, et al., 1995), SDO AIA, (Lemen et al., 2008), and H-alpha (Kanzelhoehe Observatory) space missions were also used.

Our sample of LDE flares can be characterized by the following statistical features:

—The total number of events was 72.

—The CME mass was determined for 64 (89%) of the events.
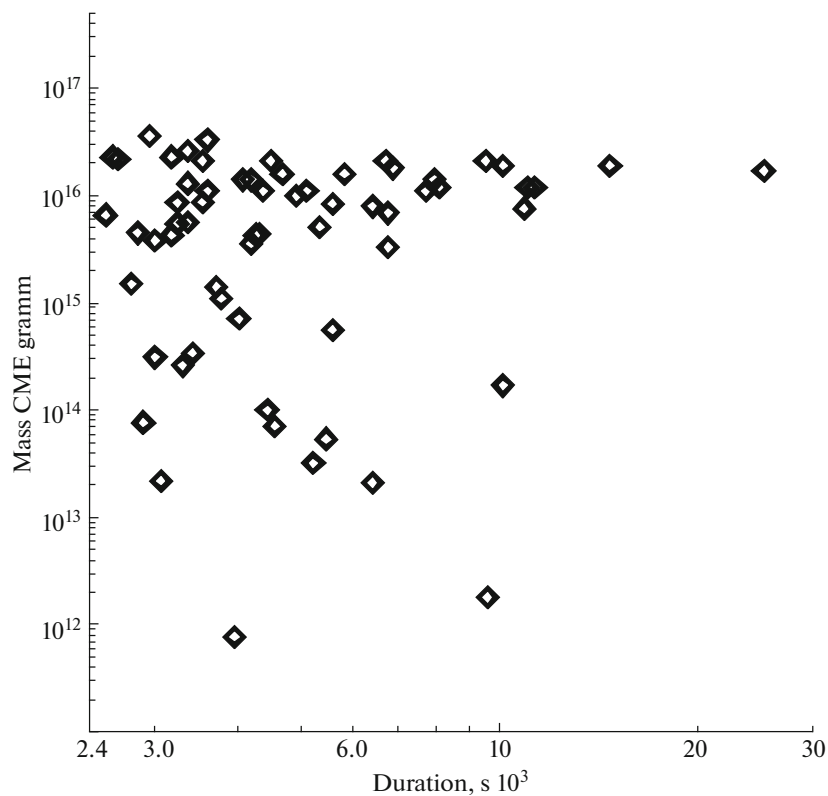
Fig. 1. Diagram of the CME mass distribution in the events of cycle 24 depending on the duration of SXR radiation of the associated the LDE flares.
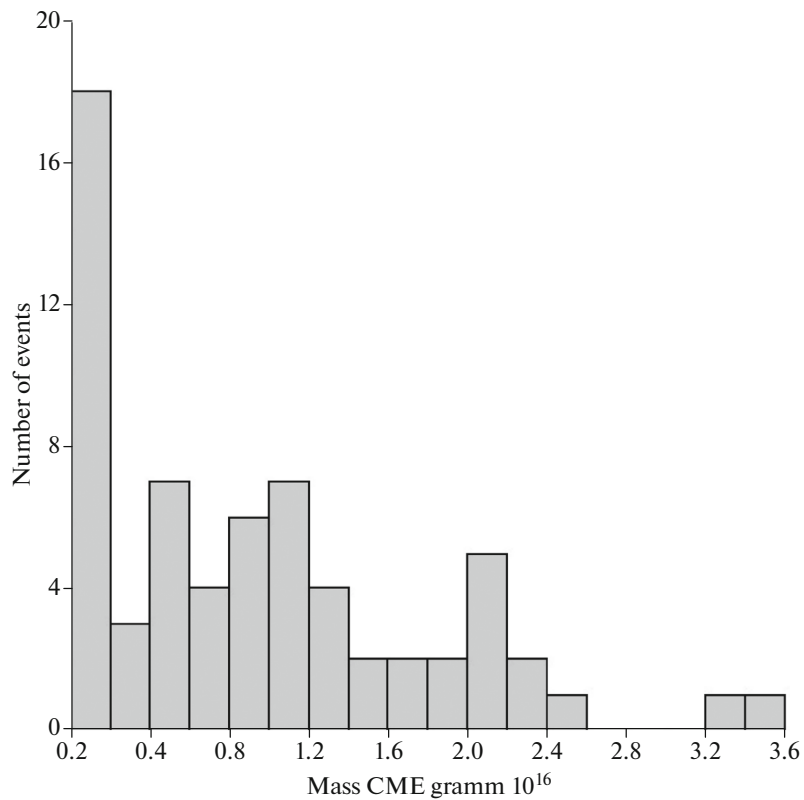
Fig. 2. Histogram of the CME mass distribution in the events of cycle 24 associated with the LDE flares.
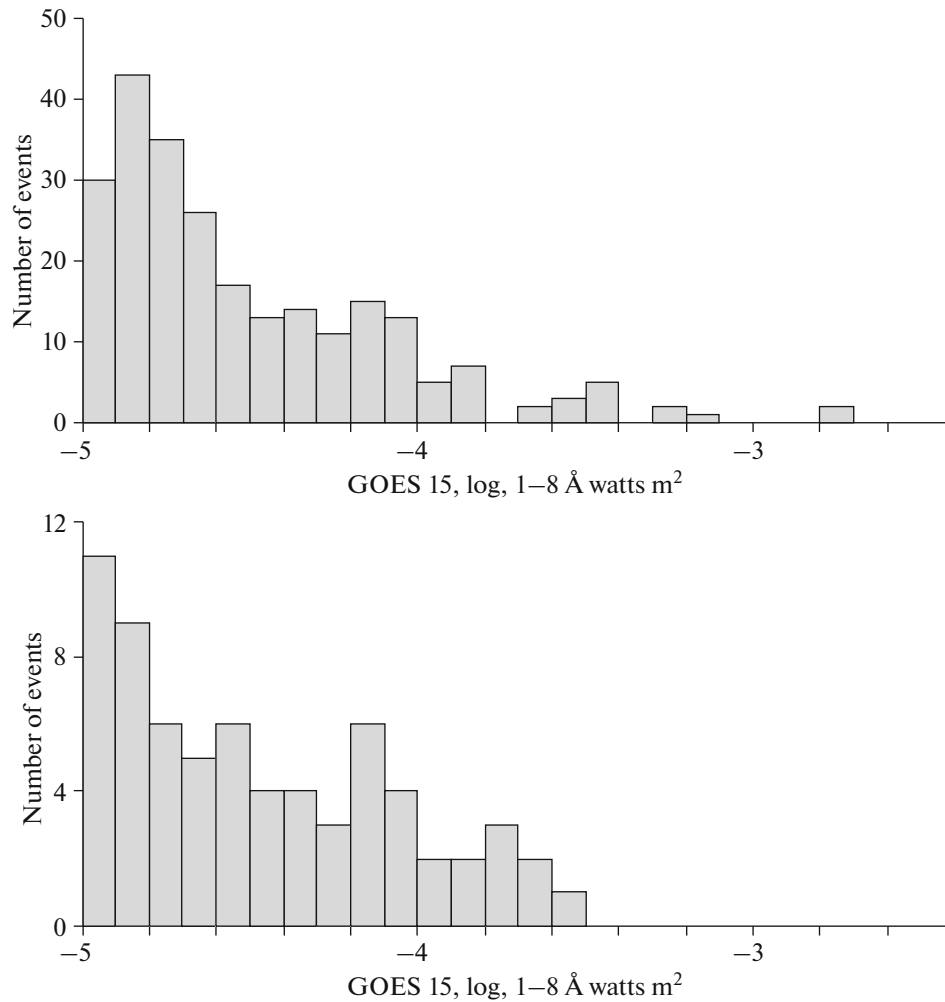
Fig. 3. Histograms of the SXR flare flux logarithm for cycles 23 (top) and 24 (bottom).

—There were 24 (33%) recurrent flares.

—CME cannibalism was observed for 12 (17%) flares.

—Several SXR peaks (GOES) were detected in 21 (29%) flares.

—EUV jets and mini-eruptions were observed in 22 (31%) flares.

—There were six (8%) flares with settling eruptions visible in the limb at 304 Å.

It can be seen from Fig. 1 that there is no clear correlation between SXR duration and CME mass, but, according to the histogram in Fig. 2, most flares are accompanied by a CME with a mass of less than 2×10^{15} g. Most LDE flares without massive CMEs occurred in October 2014.

3. COMPARATIVE CHARACTERISTICS OF LDE FLARES IN CYCLES 24 AND 23

For cycle 23, the number of LDE flares meeting our criteria was much higher, 271 events, but the SDO satellite was not yet in operation at that time, and the SOHO observations had large interruptions. Therefore, we did not study the CME characteristics but confined ourselves to the GOES15 satellite observations and studied the following parameters presented in the YYYYMMDDevents.txt files at ftp.swpc.noaa.gov/pub/indices/events/:

—Maximum SXR flux in the range 1−8 Å, during flare.

—Flare onset (first minute of 4-min monotonic SXR flux increase).

—Maximum time of SXR flare peak.

—End of flare (time accurate to the minute when the SXR flux reached the average between the maximum and background before the flare).

Based on the three latter items, we determined the following values:

—t_{dur} is the full time from the start to the end of the flare.

—t_{dur1} is the initial time phase from the flare onset to its maximum (pre-flare and impulsive phases).
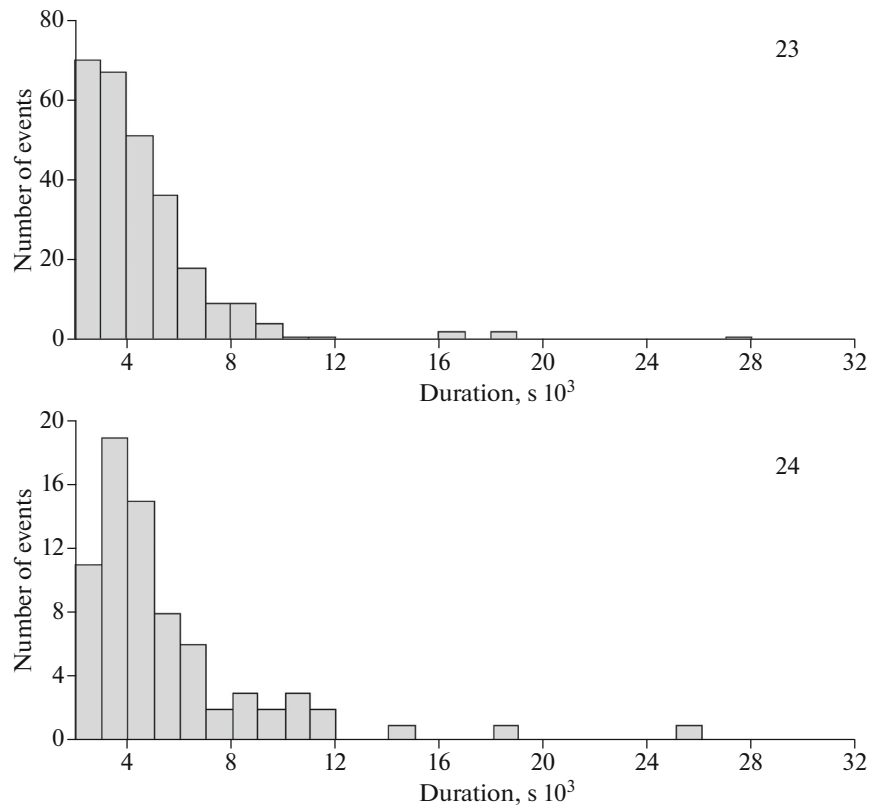
Fig. 4. Histograms of the SXR duration of the LDE flares for cycles 23 (top) and 24 (bottom).

—t_{dur2} is the decline phase of the SXR radiation (post-eruptive phase), the time from the maximum to the end of the flare.

—$a = (t_{dur2} - t_{dur1})/t_{dur}$ is the coefficient showing the ratio of flare phases.

Histograms showing the distribution of these parameters in cycles 23 and 24 were constructed (Figs. 3–5).

Figures 3 and 4 show the distribution of events by strength and duration for cycles 23 and 24. The distribution by the SXR flux for both cycles differs from the normal one; both histograms have a second maximum corresponding to M6−M8 X-ray flares. The duration distribution for both cycles is close to normal but differs in the position of the maxima. As can be seen in Fig. 4, the duration of the initial phase for most flares is more than a post-eruptive one for both cycles. This is most likely an effect from the determination of the onset and end of the flare, because the onset is not associated with the value of the maximum, and the end of the flare is associated. Figure 5 gives the distribution diagram for the SXR flux and the coefficient (*a*). Figure 6 shows the strength−duration distribution diagram for both cycles. It can be clearly seen that the selected flares of cycles 23 and 24 were limited in strength, but the straight lines limiting them differ for these cycles. Since the data in this figure are on a dou-

ble logarithmic scale, the maximum SXR flux (*F*) is a power function of duration *t*, i.e., $F = At^{-\alpha}$.

Figure 7 shows the distribution diagrams of the parameter (*a*) with respect to flare strength for both cycles. The diagram in the top panel shows that the parameter (*a*) calculated for the flares of cycle 23 is symmetrical with respect to 0 for average strength flares (from M3 to X1). For stronger flares (>X1), it is <0, i.e., these flares have a longer initial phase with the pre-flare and impulse phases. As shown in the bottom panel in the diagram of the parameter (*a*) calculated for flares of cycle 24, there is also a symmetry effect, but it is expressed more weakly because of the smaller number of flares. At the same time, the phases of the two strongest flares in the diagram (X3.1 on October 24, 2014, and X8.2 of September 10, 2017) are similar in terms of duration.

It should be emphasized that some of the strongest eruptive flares in the SXR radiation of cycle 24, e.g., X6.9 on August 9, 2011 (Sharykin et al., 2015), and X9.3 on September 6, 2017 (Struminskii et al., 2020), did not fall within the sample of LDEs. These flares had a pronounced, short, SXR impulse phase, and the SXR intensity in the long post-eruptive phase was less than half of the maximum (Fig. 8). It can also be seen in Fig. 8 based on the X9.3 event as an example that the duration of the initial phase (if the start of the event
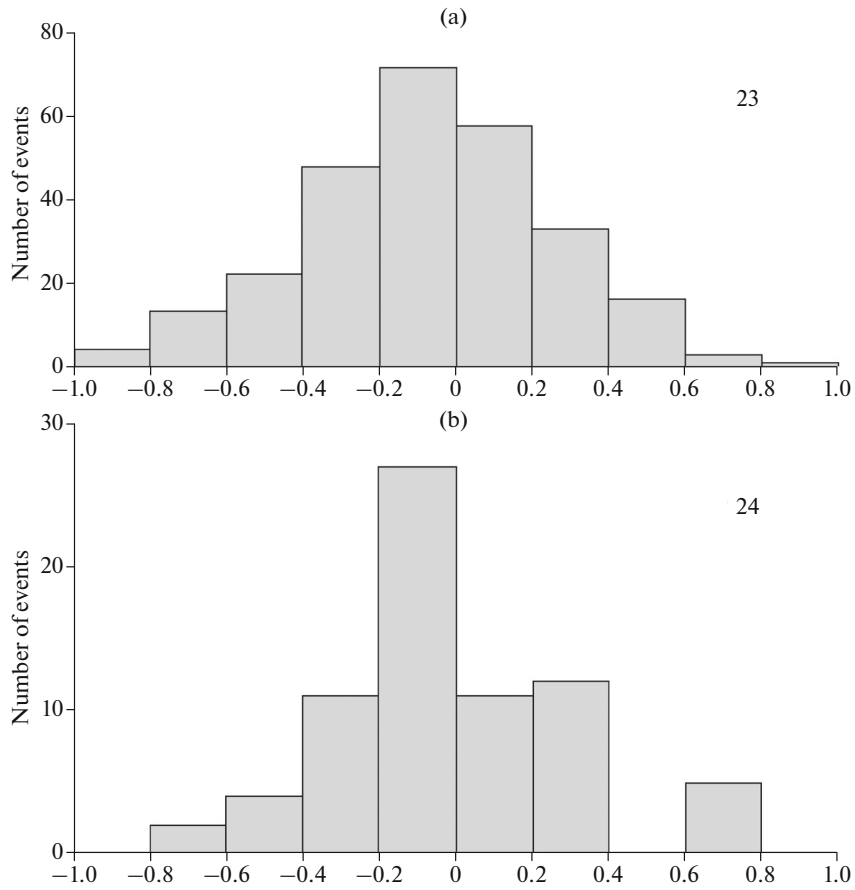
Fig. 5. Histogram of the parameter $a = (t_{dur2} - t_{dur1})/t_{dur}$ for cycles 23 (top) and 24 (bottom).
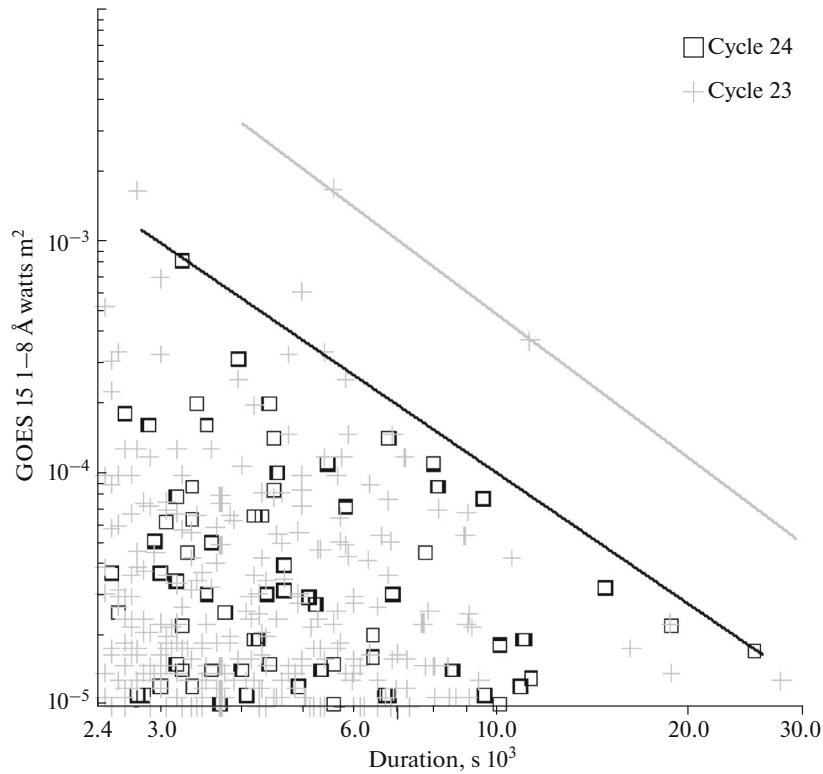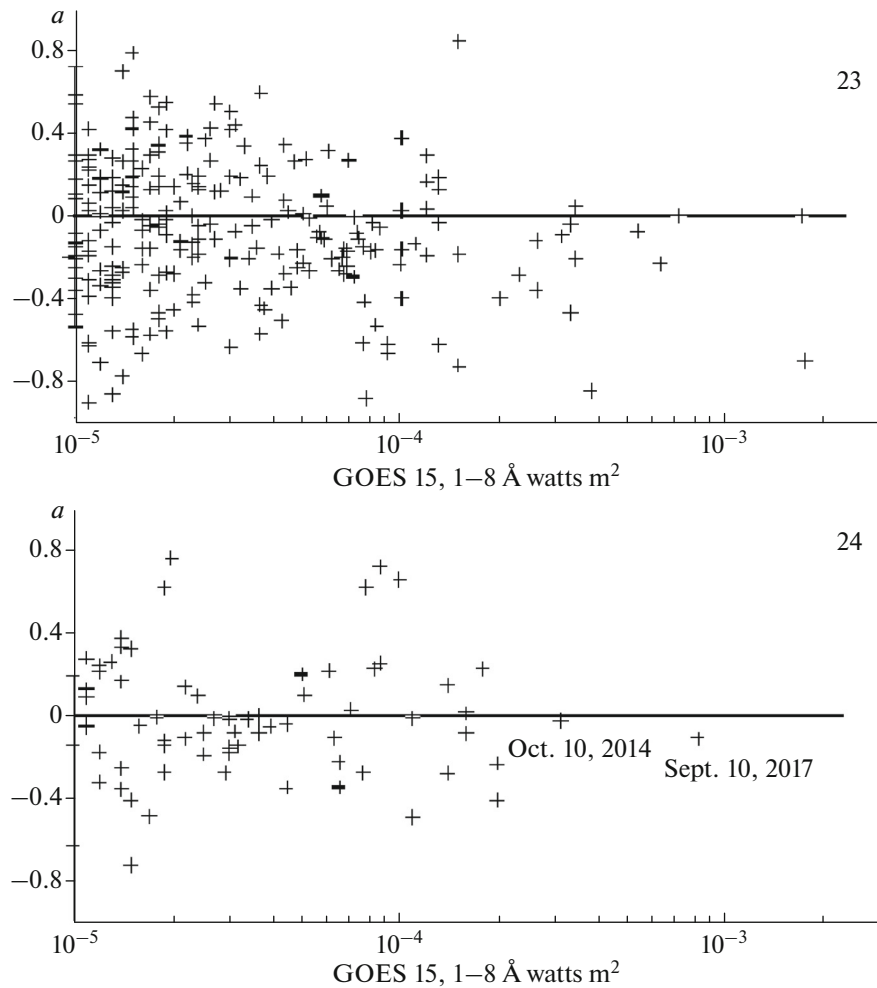

Fig 6. Diagram of strength–duration distribution. The distribution is shown by black squares in cycle 24 and by gray crosses in cycle 23. The black line limits the flares for cycle 24, and the gray line limits the flares for cycle 23.

Fig. 7. Distribution diagram of the parameter $a = (t_{dur2} - t_{dur1})/t_{dur}$ with respect to the SXR flux for cycles 23 (top) and 24 (bottom). Value 0 for the parameter (a) is marked by straight lines.

is determined) can be underestimated when a flare is detected during the decline phase of the previous one.

4. DISCUSSION AND CONCLUSIONS

No explicit correlation between mass and duration was found for the selected LDE flares of cycle 24, which contradicts the hypothesis of the role of matter settling after the CME in the development of post-eruptive flare phase, but the influence of mini-eruptions in H-alpha and EUV-jets is not improbable (Wyper and DeVore, 2016; Innes et al., 2016; Lim et al., 2016).

In our opinion, the prolonged SXR in flares is a consequence of the acceleration and chromospheric evaporation in individual post-eruptive loops. In cycle 23, there were more than three times more LDE flares than in cycle 24, because the cycle was stronger. For most of the selected flares, the initial phase was longer than the post-eruptive phase, which may indicate different variants of the development of instability

of the rope (CME) and, consequently, a different development of the acceleration processes in flares. If the rope rises slowly, more time is required to create critical instability, and impulse development is more likely if critical instability already exists.

The effect of the poste-ruptive phase duration for >X1 flares found for the parameter (a) in both cycles may be the result of the determination of the end time of the flare taken in the YYYYMMDDevents.txt files. Since the background is usually much smaller than the maximum SXR flux in the considered flares, the time of the end of the flare corresponds to a drop in the radiation intensity to half of the maximum value. In flares with a pronounced impulse phase (Struminskii et al., 2019), such a drop in the flux occurs quite quickly and is determined by the end of the effective acceleration of electrons in the impulsive phase. The decline phase in all long flares, in our opinion, is characterized by post-eruptive acceleration. The effect under discussion requires additional research.
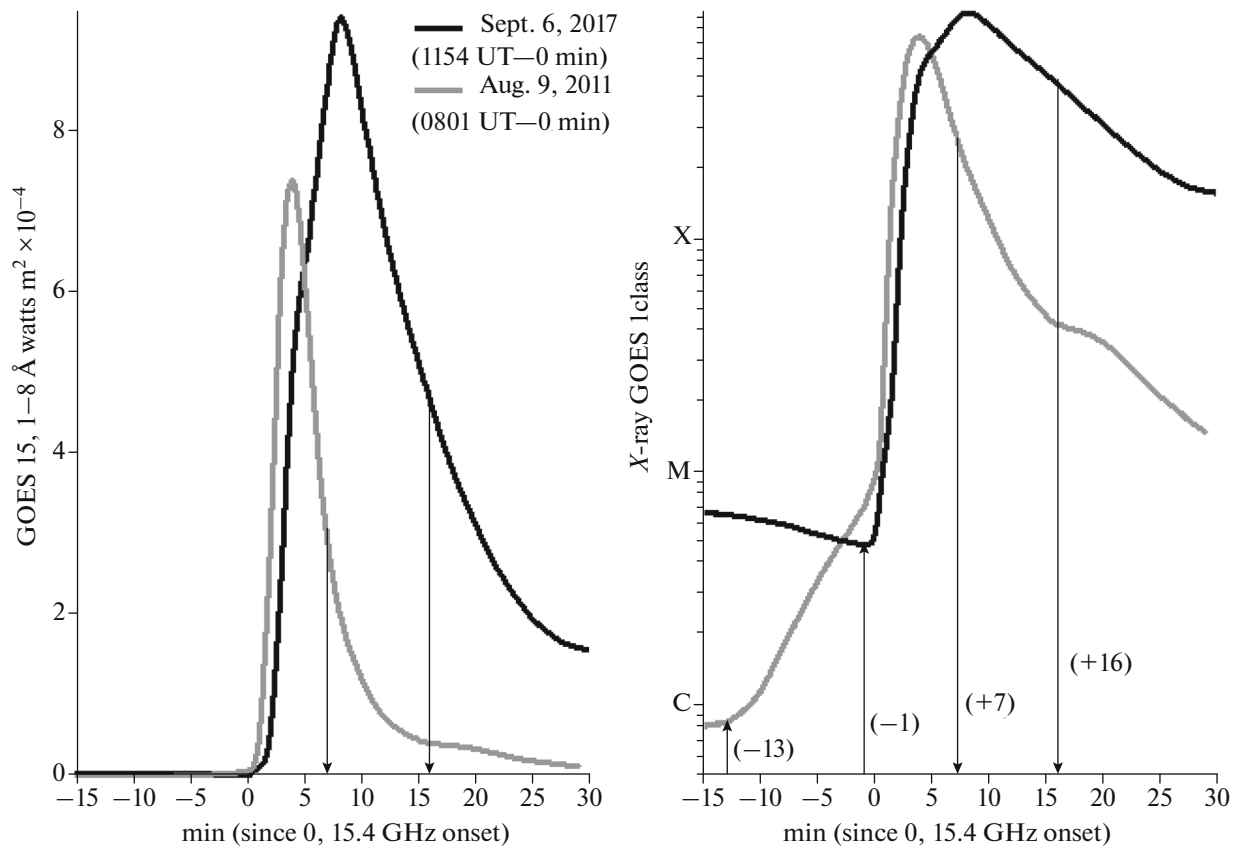
Fig. 8. SXR flux in linear (left) and logarithmic (right) scales for the flares X6.9 on Aug. 9, 2011, and X9.3 on Sept. 6, 2017, of cycle 24. The time is given relative to the onset of the SXR radiation at 15.4 GHz (see 20110809events.txt and 20170906events.txt).

Apparently, the maximum strength, which may correspond to the full flare energy, is limited (Katsova and Livshits, 2015). This limitation is different for different cycles, which, in turn, may indicate that dynamo processes are different for different cycles.

ACKNOWLEDGMENTS

FUNDING

CONFLICT OF INTERESTS

The authors declare that they have no conflict of interest.

REFERENCES

Antalova, A. and Ogir, M.B., Long-decay soft X-ray flares, *Astron. Inst. Czech. Bull.*, 1988, vol. 39, no. 2, pp. 97–105.

Brueckner, G.E., Howard, R.A., Koomen, M.J., et al., The large angle spectroscopic coronagraph (LASCO), *Sol. Phys.*, vol. 162, nos. 1–2, pp. 357–402.

Gopalswamy, N., Coronal mass ejections: Initiation and detection, *Adv. Space Res.*, 2003, vol. 31, no. 4, pp. 869–881.

Innes, D.E., Bučík, R., Guo, L.-J., and Nitta, N., Observations of solar X-ray and EUV jets and their related phenomena, *Astron. Nachr.*, 2016, vol. 337, no. 10, pp. 1024–1032.

Katsova, M.M. and Livshits, M.A., The origin of superflares on G-type dwarf stars of various ages, *Sol. Phys.*, 2015, vol. 290, no. 12, pp. 3663–3682.

Lemen, J.R., Title, A.M., Akin, D.J., et al., The *Atmospheric Imaging Assembly* (AIA) on the *Solar Dynamics Observatory* (SDO), *Sol. Phys.*, 2008, vol. 275, nos. 1–2, pp. 17–40.

Lim, E.-K., Yurchyshyn, V., and Park, S.-H., Observations of a series of flares and associated jet-like eruptions driven by the emergence of twisted magnetic fields, *Astrophys. J.*, 2016, vol. 817, no. 1, id 39.

Livshits, M.A., Belov, A.V., Shakhovskaya, A.N., et al., Coronal mass ejections in July 2005 and an unusual heliospheric event, *Cosmic Res.*, 2013, vol. 51, no. 5, pp. 326−334.

Shakhovskaya, A.N. and Akhtemov, Z.S., The relationship between the duration of solar X-ray flares and the mass of associated coronal ejections, *Bull. Crimean Astrophys. Obs.*, 2013, vol. 109, no. 1, pp. 86−89.

Shakhovskaya, A.N., Livshits, M.A., and Chertok, I.M., The role of plasma ejections in the development of large solar flares of various durations, *Astron. Rep.*, 2006, vol. 50, no. 12, pp. 1013−1025.

Sharykin, I.N., Struminskii, A.B., and Zimovets, I.V., Plasma heating to super-hot temperature (>30 MK) in the August 9, 2011 solar flare, *Astron. Lett.*, 2015, vol. 41, nos. 1−2, pp. 53−66.

Shibasaki, K., Energy and mass supply in the decay phase of long-duration solar flare events, *Astrophys. J.*, 2002, vol. 567, no. 1, pp. L85−L87.

Struminskii, A.B., Logachev, Yu.I, Grigor'eva, I.Yu., and Sadovskii, A.M., Two types of long-term flares: solar protons and relativistic electrons, in *Trudy XXIII konf. "Solnechnaya i solnechno−zemnaya fizika-2019"* (Proc. of the XXIII Conf. "Solar and Solar−Terrestrial Physics-2019"), Moscow: GAO RAN, 2019, pp. 377−380.

Struminskii, A.B., Grigor'eva, I.Yu., Logachev, Yu.I., and Sadovskii, A.M., Solar electrons and protons in the events of September 4−10, 2017 and related phenomena, *Plasma Phys. Rep.*, 2020, vol. 46, no. 2, pp. 176−190.

Wyper, P.F. and DeVore, C.R., Simulations of solar jets confined by coronal loops, *Astrophys. J.*, 2016, vol. 820, no. 1, id 77.

Yashiro, S. and Gopalswamy, N., Statistical relationship between solar flares and coronal mass ejections, *Proc. Int. Astron. Union Symp.*, 2009, vol. 257, pp. 233−243.

Translated by O. Pismenov